Local Ionization in 2-Phenylethyl-*N*,*N*-dimethylamine: Charge Transfer and Dissociation Directly after Ionization

R. Weinkauf*

Institut für Physikalische Chemie und Elektrochemie, Heinrich Heine Universität, Düsseldorf, Universitätsstrasse 1, 40225 Düsseldorf, Germany

L. Lehr†

Institut für Physikalische und Theoretische Chemie, Technische Universität München, Lichtenbergstrasse 4, 85747 Garching, Germany

A. Metsala

Institute of Chemistry at Tallinn Technical University, Akadeemia tee 15, 12618, Tallinn, Estonia

Received: May 1, 2002; In Final Form: September 25, 2002

The 2-phenylethyl-*N*,*N*-dimethylamine (PENNA) radical cation offers two functional groups for a positive charge to reside, the benzyl ring and the substituted amine group. Previously published HeI photoelectron spectra (PES) and our B3LYP data of the cation ground state agree that the amine site has the lowest ionization energy (IE). In this work we present evidence that by resonant laser multiphoton ionization the electron is removed from the phenyl site. B3LYP calculations of the neutral molecule predict that by far the most stable structure is the nonsymmetric unfolded anti conformer and that no other conformer should be significantly populated. This is confirmed by the S_0-S_1 resonant two-photon ionization (R2PI) spectrum in which one conformer is found to be predominant. The presence of the vibrational fingerprint of the phenyl chromophore and the absolute energetic position of the R2PI spectrum clearly show the local character of the first photoexcitation. Surprisingly, the R2PI mass spectra taken via S_1 resonances show strong fragmentation. The parent-to-fragment-ion ratio is about 1:10 and mostly independent of laser intensity. The metastable character of the decay excludes a fragmentation caused by cation photoabsorption. The strong dissociation directly after ionization is explained by (i) a local ionization at the phenyl chromophore, (ii) a fast charge transfer (CT) to the lower-energetic amine site, and (iii) a subsequent metastable dissociation. A first detailed analysis of the ionization process indicates that intersite R2PI ionization between local states is a one-photon two-electron process which is expected to be improbable and that a failure of local ionization only happens in cases of mixed intermediate S_1 states or mixed cation states. PENNA with two possible charge sites spaced by a $-CH_2-CH_2-$ bridge is an ideal model system to study the dynamics of a downhill charge transfer after local ionization to the first excited cation state as presented in a forthcoming paper.

I. Introduction

Properties of small molecules are experimentally and theoretically reasonably well-understood. As for large and ultralarge molecules, a global description on high experimental and theoretical levels is difficult and a local model was introduced: It is assumed that in large molecules functional groups (here termed "sites") which are spaced by saturated carbon bridges only weakly interact. This assumption is based on the observation that functional groups in different molecules have very similar physical properties. For example, concerning photoabsorption, the benzyl group behaves similar in a peptide as in isolated *n*-propylbenzene or the amine group in a peptide N terminal similar as in ethylamine. Naturally the local properties of the sites are slightly modified by nearby substitutions and the solvent environment. For example, the changes in fluorescence lifetime or frequency of the indole chromophore of the amino acid tryptophan have been used for peptide structural analysis.[1] Despite such small modifications, the local model is a suitable and very helpful approximation which allows access to large and ultralarge neutral molecules.

Later the model of local sites was also widely applied to large charged systems in solution. In gas phase so far the application of a local approximation is sparse and up to now was used only for some molecules[2−4] and clusters.[5−7] Presumably the reason for this is that only few large molecules have been investigated up to now in gas phase. The results of theses papers[2−7] are based on the assumption that a resonant two-photon ionization (R2PI) via a neutral, local S_1 state also forms a local charge distribution in the cation. The energetics of the charge at different molecular sites (for molecules) or molecules (for clusters) was described by local ionization energies (IEs) of the functional groups. For determination of local ionization energies helium photoelectron spectra (HeI PES) of model molecules, such as amino acids,[8,9] neurotransmitters,[10] or functional groups[11] proved to be helpful.[4]

In heteromolecular clusters, charge transfer (CT) between molecules was indirectly observed by delayed ionization[5] or

* To whom correspondence should be addressed.
† Present address: Accenture GmbH, Maximilianstraβe 35, D-80539 München, Germany.

10.1021/jp021092c CCC: $25.00
Published on Web 03/29/2003

fragmentation.[6] Because the local ionization was not the main focus of these investigations, no further experiments were carried out to prove the local character of the ionization step or the cation states. The same holds also for most of the other experiments. Levy and co-workers[2] and later Weinkauf et al.[3,4] also used the local model for investigation of CT in extended molecular cations. Levy's group monitored the CT directly after ionization in various synthetic two-site donor-bridge-acceptor systems,[2] In this investigation, carried out with nanosecond laser pulses, it was not possible to detect the charge in the site of neutral excitation and local ionization. This was interpreted as an ultrafast CT after ionization. In this work, however, an alternative explanation by a direct ionization to the second site of lowest IE was not fully excluded. Weinkauf at al. initiated and probed photoinduced CT in excited states of a series of model peptide radical cations under isolated conditions.[3,4] In these experiments[4] an effective photoabsorption of visible light (VIS) by peptide cations was detected by fragmentation. This VIS photoabsorption is typical for charged aromatic chromophore, a clear indication for the validity of the local IE model and the local ionization in aromatic chromophores in peptides. In contrast to the two-site molecules investigated by other groups,[2,5−7] peptides are multisite systems. One new aspect for cations of large extended molecules in comparison to small molecules is that electronic states can be localized at different sites and more importantly the energy differences between electronic states might be small or even vanishing.[3,4] This is in sharp contrast to neutral molecules where S_1 absorptions of aromatic chromophores are typically energetically well-separated from the electronic states of nonaromatic functional groups.

There is up to now only one example in the literature where in gas phase the local IP model was combined with solvation:[7] Local ionization and subsequent charge transfer (CT) was made responsible for fragmentation in amphetamine, 2-phenylethylamine (PEA), and their clusters with polar solvents.[7] Using experimental and theoretical data we found previously, however, full charge delocalization after ionization for the above PEA.[12,13] PEA has two energetically degenerate sites spaced by a $-CH_2-CH_2N-$ bridge. In PEA therefore despite a local S_1 excitation the local ionization fails (see below).

There are other cases for clusters where a local model also fails. For example, in stacked cation dimers the surplus charge is found to be equally delocalized over the two units leading to a binding energy of up to 0.5 eV[14,15] and to mixed, global, bonding and antibonding states with a state splitting of about 1 eV. This huge effect is termed "charge resonance" (CR). Beside homo dimers CR has been observed for hetero-molecular dimers with similar IEs.[16]

In conclusion, for molecules and clusters there might be cases where ionization is local and cases where local ionization fails. The local character of the states is correlated with energetics and coupling of the two sites. Clearly local ionization is guaranteed if (i) there is a suitable chromophore with a high S_0-S_1 transition moment, an IE which is by far the lowest in the system and (ii) the two-photon energy of the resonant laser is just sufficient to ionize at this site, but not elsewhere. If conditions (i) to (iii) are fulfilled a suitably low two-photon energy enforces a site-selective ionization. There is simply no alternative excitation route accessible. This was the scheme we used previously for our CT investigations on peptides (note that we did not used phenylalanine in our model peptides because the IE of phenyl is about equal to the IE of the N terminal).[4]

The question we address in this work is, what happens in a two-site molecular system, if the excited chromophore has the higher IE? In this case the system has energetically the choice to ionize at a second site. The question is whether excitation via the local S_1 state is then still local in the same chromophore, or would ionization lead to the lowest energy site outside the chromophore (intersite ionization) or to a fully mixed state of the cation? This question can nor be easily answered because up to now it is not clear which energy mismatch of two $-CH_2-CH_2-$ spaced sites is needed to have local character. In total we will show that in PENNA the two sites are local and that it is a model system to test CT dynamics directly after ionization (see also our forthcoming paper[17]).

Its worth noting that mass spectrometry experiments with local ionization are sparse. Conventional ionization techniques are not able to form radical cations with a site- or energy-selective charge distribution. Therefore, although in mass spectrometry the possibility of charge transfer has been already discussed,[18] so far no direct experimental results exist.

II. The Concept of Local Ionization: An Analysis

Local ionization is clearly the precondition for investigation or detection of CT in molecular[2−4] and cluster cations.[5−7] As mentioned above, it is so far not investigated in detail. In the following we analyze the concept of local ionization on the basis of molecular orbitals.

Assume for the following that the local site model holds equally for neutrals and cations. One then can define for a two-site molecule two sets of local molecular orbitals (MOs) and local electron populations for the neutral ground, the S_1, the cation ground, and its excited states (Figure 1 insets). The basic idea of local ionization is a preselection of the ionization site by a local S_0-S_1 photoexcitation. We assume in the following for simplification that S_1 has a local and unmixed MO configuration where one electron is excited from the highest molecular orbital (HOMO) into the lowest unoccupied molecular orbital (LUMO) of an aromatic chromophore. This assumption is reasonable because often aromatic and nonaromatic neutral sites have very different electronic energies and are weakly coupled. Photoionization at the site of first photon excitation then is just a removal of the already excited electron (Figure 1, site 1, full arrow). From the S_1 state this is an allowed one-photon one-electron process. Ionization to the second local site with its own local MOs, (site 2 in Figure 1) would be (i) an intersite and (ii) a one-photon two-electron excitation (Figure 1, dotted arrow).

Up to now there are few experimental indications of "intersite photoionization". We therefore judge its feasibility from other related experiments. One hand-waving argument for a weak transition moment for intersite transitions would be a possible small spatial overlap of the local electronic wave functions. Surprisingly, very strong optical CT transitions have been observed in clusters cations.[19,20] Moving the charge center from one site to an other just by photoexcitation seems to be no problem, at least if the intersite distance is not large. An analysis shows that in these examples the transitions were one-photon one-electron processes.[19,20]

A preferential selection rule that one-photon one-electron transitions are much more probable than one-photon two-electron transitions is well-known from vacuum ultraviolet (UV) photoelectron spectroscopy (PES) of molecules in their neutral ground states.[21] As for multiphoton ionization, in conjugated "one-site" molecules Stolow and co-workers[22,23] achieved selective electronic state population in the cation. They used R2PI via suitable intermediate states for state selection and PES for detection of the cation electronic state population (Note that such a direct proof is still missing for local ionization of large

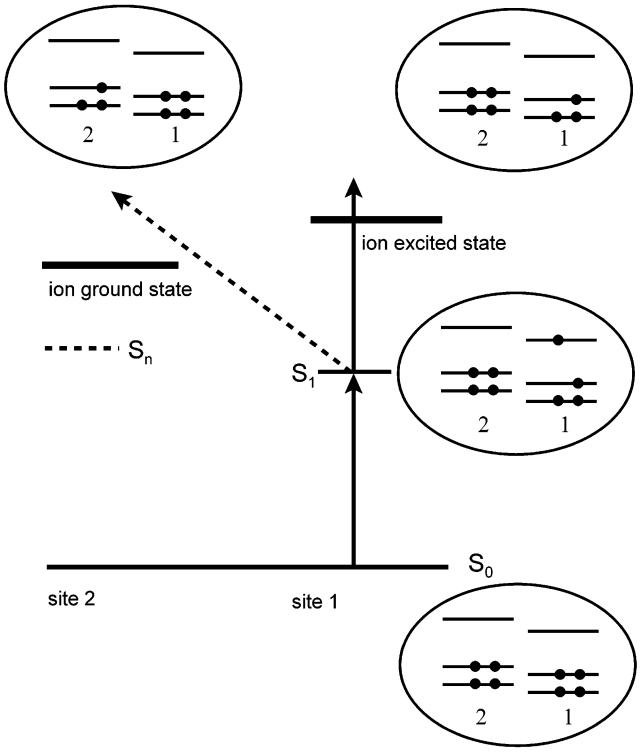

Figure 1. According to the local model for large molecules, local neutral and cationic electronic states and their schematic local molecular orbital populations are shown. The basic idea for local laser ionization is a pre-selection of the ionization site (site 1) by a local S_0-S_1 excitation. If S_1 at site 1 has an unmixed, local MO configuration where one electron is excited from the highest molecular orbital of site 1 into the lowest unoccupied molecular orbital of site 1, ionization at the same site is just a removal of the already excited electron (full line arrow). From S_1 this is a one-photon one-electron process. Ionization from this S_1 to a different local site (site 2) would be then a one-photon two-electron process (dotted arrow). Up to now there exists no evidence for "intersite ionization" processes, but there are arguments that they might be weak (see text). As shown in this work this local ionization and cation energy scheme holds also for PENNA.

extended molecules). In their experiment the electron configuration of the intermediate state, by one-photon one-electron ionization, converged to the ground or an excited state of the cation. One-photon two-electron excitations were found to be weak. One can assume that this preferential one-photon one-electron selection rule is transferable to extended molecular systems. Still, so far, a direct proof that one-photon two-electron intersite excitations are weak is missing. The work of Stolow and co-workers[22,23] also showed that for intermediate states with mixed MO configurations the steering of cation electronic state population fails. A second source of intersite excitation can be a state coupling in the ion. From one-photon PES it is well-known that mixing by configuration interaction can take place in the final cation electronic state.[21]

In the following we confine our discussion in this paper to the two complementary reasons why R2PI could fail to be local:

(i) a nonnegligible transition moment for intersite ionization between local neutral and local cation states and

(ii) a strong intersite coupling in the cation leading to a full mixing of the two sites.

(i) In this work, the lack of an intersite excitation will be proven experimentally for PENNA. In the two-site molecular model systems used up to now, such as *n*-alkylbenzenes,[24] *n*-phenylethanole,[12,13] propionic acid,[12] and model peptides,[3,4] the aromatic chromophore had by far the lowest IE. In these experiments the resonant two-photon ionization offered enough energy for efficient ionization at the chromophore (IE $< 2h\nu$) and two-photon ionization at any nonaromatic site was, however, energetically improbable, because a process of higher order (IE $> 2h\nu$). In this work we investigate the reverse case where ionization to the nonaromatic site is the lowest energetic route.

(ii) As mentioned there are cases where a local model fails.[13−16] Besides local orbital size and their relative orientation, the intersite coupling strength in molecules is dependent on their energetic difference and the molecular bridge. The bridge-induced coupling is given by its length and its nature as well as the type of bonding to the sites. In CT theory "through space" and "through bond" effects are distinguished. The later is defined as CT through a bridge which is valence-bound to both sites. Halpert and Orgel (conjugated bridges[25]) and also McConnell (saturated carbon bridges[26]) theoretically investigated the bridge-induced electronic coupling between two sites. This concept was elaborated and quantitatively tested by Reimers and Hush[27] and later developed to the "superexchange CT model".

Clearly a local approximation is only a good model when the coupling between the local sites is small.[26,27] With increasing intersite coupling an oscillatory motion of the charge between the two sites is found.[27] For strongly coupled isoenergetic sites the charge motion is calculated to take place on an electronic time scale ($\tau < 20$ fs).[27] In conventional ns laser pulse experiments this can only by observed as a time-averaged charge delocalization. To generate the global wave functions the local wave functions were superimposed to create symmetric (+) and anti-symmetric (−) linear combinations which are split by the intersite coupling.[14−16,26,27] Knowing the local IEs of the functional groups, the splitting or shifting as caused by the coupling can be identified in the PE spectrum of the two-site molecule. Hence, such deviations from the local model contain information about the intersite coupling strength (see below).

Above considerations only take into account electronic effects. The nuclear motion is not included[26] or implemented as a damping.[27,28] Complex and detailed influences of conformational changes or individual reaction coordinates might be important but are difficult to include.

III. 2-Phenyl-*N*,*N*-phenylethylamine (PENNA): Evidences for Local States

In our search for a model molecule we looked for a functional group which has a lower IE than the phenyl chromophore. As mentioned above, charge delocalization over two energetically degenerate charge sites is found in PEA,[13] a basic chemical structure for neurotransmitters.[28] HeI PES of PEA and substituted analogues show two close-lying, partly overlapping electronic bands clearly correlated to the presence of the phenyl and the amine groups.[10] One-photon ionization of the *N*,*N*-dimethyl-substituted PEA (PENNA) leads to an electronic state which is lower in energy than the typical IE of the phenyl group. This cation ground state shifts upon stepwise CH_3 substitution at the amine.[10] In contrast within the experimental resolution the second band is not affected by this substitutions. This shifting upon substitution was used for the identification of the bands on the basis of a local model.[10] The first band is assigned to ionization at the amine and equivalently the second band to ionization at the phenyl chromophore. In the following we provide further supporting arguments for this assignment. One experimental fact is the large splitting between the two states of about 0.7 ±0.2 eV in PENNA,[10] which could have two reasons:[26,27] (i) The local IEs of the isolated functional groups

TABLE 1: Calculations of the Five Conformers of Neutral 2-Phenyl-*N,N*-dimethylamine (PENNA) Using Various ab Initio and Density Functional Methods and Different Basis Sets[a]

	conformer				
method	**I**, gauche lone pair$-\pi$	**II**, gauche $CH_3-\pi$	**III**, gauche $CH_3-\pi$	**IV**, nonsymmetric anti	**V**, symmetric anticonformer
MM3	59	626	535	0	318
HF/6-31+G(d)	439	1230	439	0	345
MP2/6-31+G(d)	33	566	137	0	431
MP3/6-31+G(d)[b]	213	815	420	0	433
MP3/6-31+G(d)[c]	234	848	530	0	446
PW91/6-31+G(d)	395	1027	731	0	259
B3LYP/6-31G(d)	218	817	660	0	171
B3LYP/6-31+G(d)	391	1082	741	0	312
B3LYP/6-311+G(d)	338	1023	692	0	294
B3LYP/6-31+G(d)+ZP[d]	365	1085	746	0	314
B3LYP/6-31+G(d)+G_{300}[e]	259	1256	800	0	300
B3LYP/6-31+G(d)+G_{360}[f]	226	1282	801	0	288

[a] If not explicitly marked, all values result from full geometry optimization methods. For B3LYP 6-311+G(d) structures, see Figure 2. The conformer numbering is chosen in analogy to 2-phenylethylamine (PEA).[13] All methods and levels of theory agree on the nonsymmetric anti conformer (conformer **IV**) to be the most stable conformer. MM3 is included because it is widely used for large molecules and can be compared here to other methods. B3LYP and PW91 agree with the experimental result (Figure 6) of a strong thermal population of one conformer, but interestingly not MP2. The comparison of experimental data and theory is performed in section V.3. Energies are relative energies in respect to the lowest conformer and are given in cm^{-1}. [b] Single-point calculation using the MP2 6-31+G(d) geometry as input. [c] Single-point calculation using the B3LYP/6-311+G(d) geometry as input. [d] ZP includes vibrational energy. [e] G_{300} includes the Gibbs free energy at 300 K (accounting for differences of density of states in the different conformers. [f] G_{360} includes the Gibbs free energy at the nozzle temperature of 360 K (accounting for differences of density of states in the different conformers).

are similar and their coupling in PENNA is strong, leading to a large splitting of the + and − linear combinations in the two-site molecule or (ii) the states are very weakly coupled and local and just energetically different. The methyl substitution experiment[10] favors explanation (ii). In the following we present further arguments to exclude explanation (i).

As mentioned the differences of the state energies in the composed molecule versus the isolated functional groups are criteria for the degree of the intersite coupling and therefore the degree of charge localization. If the isolated versus composed agreement is good, the states are weakly coupled and in good approximation local. The agreement between the first IE of PENNA (7.8 eV[10]) and the IE of trimethylamine (8.0 eV, onset in ref 11) is relatively good. The remaining difference may be partly explained by a further lowering of the IE in PENNA due to the longer alkyl chain in comparison to trimethylamine. In analogy to the length-dependent IE shift observed in alkylbenzenes[24] this would account for a lowering of about ∼0.14 eV. The remaining small difference of 0.06 eV lies within the error to determine the electronic origin transition:[10] Typically HeI PE spectra are recorded at temperatures of or above room temperature leading to thermal population of especially low-frequency modes and hot-band transitions. Trimethylamine for example has already a high vapor pressure at room temperature. In contrast PENNA has to be heated to about 360 K. It also has a lot of low-frequency vibrations so that hot-band transitions which are shifted to lower energies than the origin transition cause an onset of the He I PE spectra[11] at energies lower than the origin transition. Our IE value of PENNA, however, corresponds to the onset of the HeI PES and therefore might be too small. This systematic error could account for the remaining small difference between the local IEs and the IE in PENNA. In conclusion the local IE approximation seems to hold well for PENNA.

The IE of the excited electronic cation state of PENNA is difficult to determine.[10] Within the experimental error it does not shift in respect to *n*-butylbenzene (aa conformer: 8.675 eV[24]). If we accept the local approximation also to hold for this excited cation state, we estimate an energy of 8.5 eV for the second IE. For this estimation we use the IE shifts observed in *n*-alkylbenzenes as caused by increase of the molecular size.[24] Note that due to the extended structure self-solvation by folding is excluded (see below).

To summarize, we have a coherent picture which supports that in PENNA cations the first two bands are local states (Figure 1). From literature data and our previous experiences we expect that in the electronic ground state the charge is mostly stored at the amine group (see chapter IV) and that about 0.7 eV higher in energy the first electronic excited state has a preferential charge localization at the phenyl site.

IV. Calculations

In the following we present theoretical calculations for the neutral and cationic PENNA. The aims are (i) to obtain indication for the conformational structure of the neutral molecule and (ii) to gain information about the degree and site of charge localization in the cation ground state. The calculations were performed with the Gaussian 98 program package.[30] To our knowledge these are the first calculations of the conformational structures of neutral and cationic PENNA.

IV.1. Calculations of Neutral PENNA. To our knowledge these are the first calculations of the conformational structures of PENNA and their cationic electronic structure. Due to the different site-to-site distances, the conformer classes "folded" and "linear" may have different coupling mechanisms, namely "through space" or "through bond". Therefore we need to know the preferential structure of PENNA to clarify the type of coupling. Because of the relatively large size of PENNA, if one chooses accurate theoretical methods, such as MP2, as a consequence the basis set size is small and if one chooses a large basis set the only method which is still possible might be not well-tested. We therefore rely on a broad variety of methods and try to become additional confidence by variation of the basis sets: HF, MP2, and single-point MP3 *ab initio* as well as PW91 and B3LYP density functional calculations with basis sets 6-31+G(d) and partly 6-311+G(d) were carried out for all stable conformers of neutral PENNA. To find all local minima, the conformational landscape was explored using a program named Tinker.[31] In Table 1 the results of calculations of different levels and methods for all five PENNA conformers are presented. To

TABLE 2: Some Theoretical Results for Neutral PEA for Comparison to Table 1[a]

	conformer				
method	**I**, gauche lone pair−π	**II**, gauche H−π	**III**, gauche H−π	**IV**, nonsymmetric anti	**V**, symmetric anti
MP2/6-311++G(d, p)[b]	731	115	0	468	489
MP3/6-311++G(d, p)[c]	623	68,5	0	238	291
B3LYP/6-311+G(d, p)[d]	518	30	0	86	42

[a] Four comparably thermally populated neutral PEA conformers have been found in the experiment (see R2PI spectrum in inset of Figure 6). Note the qualitative agreement of the number of populated conformers between the experiment and the B3LYP result. For PEA and PENNA conformers **I**, **II**, **III**, and **IV** are 2-fold degenerate. [b] Reference 34. [c] This work: single point calculation, using the MP2 geometry of ref 34. [d] Reference 13

allow easy comparison only the relative energies with respect to the lowest conformer are given. The B3LYP 6-311+G(d) structures and their relative energies are presented in Figure 2. The conformer numbering in Figure 2a,b agrees with previous nomenclature.[13] Note also the numbering of the relevant atoms in Figure 2a, conformer **I**. We distinguish between conformers formed by rotation along the C3−C2 axis (2a gauche, 2b anti). Within the families of gauche and anti structures further structural varieties are formed by rotation of the methylated amine group about the N1−C3 axis. The comparison between our calculated and experimental data is performed in section V.3. With the B3LYP/6-31+G(d) method we also explicitly searched for "planar" structures by setting the dihedrical angle ϕ(C6,C1,C2,C3) equal zero, but only found saddle points about 600 cm^{-1} above the nonplanar stable conformers ($\phi = 90°$).

The existence of five stable rotamer structures for PENNA agrees well with the five minima for the nonmethylated species PEA.[7,13,32−34] For comparison to PENNA (Table 1) the existing calculations of PEA are shown in Table 2.

With B3LYP four conformers of PEA lie within an energy range of 100 cm^{-1} in good agreement with the experimental observation of four thermally populated conformers. MP2, B3LYP, and single-point MP3 calculations agree that the folded gauche rotamer **III** with a CH−π interaction is the (lowest-energetic) structure. Surprisingly, MP2 calculations do not agree with a comparable thermal population of four conformers, but relative conformer energies of single-point MP3 and B3LYP calculations do note that the isomerization barriers for PEA are high (for example, the isomerization from conformer **V** to conformer **IV** is 891 cm^{-1}) and the thermal population in the nozzle is expected to be not very much changed by the supersonic expansion (see section V.3).

The relative conformer energies of PEA and PENNA are very different (Tables 1 and 2). For PENNA (Table 1) all methods agree on the nonsymmetric anti conformer to be the most stable structure. Comparing the nonsubstituted and the substituted molecules this switch in stability from a folded to an extended conformer is presumably due to steric hindrances between the CH_3 group and the π system. This accounts especially for conformers **II** and **III** where the $-CH_3$ group is close to the chromophore (Figure 2a). Similar to PEA, also in PENNA the nitrogen lone pair-to-π interaction for the folded conformer **I** is repulsive. For PENNA this effect is, however, somewhat smaller than for PEA. Therefore in PENNA conformer **I** could have some population at the nozzle temperature of 360 K (section V.3). Concerning the extended conformers the higher stability of conformer **IV** in comparison to that of conformer **V** might be also a steric effect (see Figure 2b, conformer **V**).

In total all calculations conducted on different levels and with different methods agree that the most stable structure of PENNA is the nonsymmetric anti conformer. Note that this conformer is the only one which is not twice degenerate.

Concerning structural assignment the only experimental evidence we have is the relative intensities of the conformers in the R2PI spectrum (section V.2). In section V.3 we try to correlate the calculated data to the experiment and show that this comparison is convincing enough for a reliable identification of the most stable conformer of PENNA.

For PENNA the large change from the HF to the MP method should show the influence of the electron correlation between the two sites, favoring the gauche over the anti structure (Table 1). The MP2 results of two nearly equally stable conformers (**I** and **IV**) are, however, in contrast to the predominant appearance of one conformer in the R2PI spectrum. One could assume that for the relatively small 6-31+G(d) basis set still the basis set superposition error (BSSE) is contributing an artificially stronger intersite binding for the gauche conformers. Going to a larger basis set could reduce this, but no large net effect would be expected because the closer intersite electron distance allowed by the larger basis set would also result in more correlation attraction. Interestingly single-point MP3 calculations using the MP2 and the B3LYP geometries significantly differ from MP2. They considerably reduce the stability of the folded conformers and distinctly favor conformer **IV**. This is in good agreement with the observation of one predominant conformer (sections V.2 and V.3). As in PEA, MP2 seems to overestimate the intersite electron correlation. In contrast to this, density functional methods are well-known to underestimate the intersite electron correlation. PW91 and B3LYP results with a 6-31+G(d) basis set agree very well, indicating that for the two methods the intersite electron correlation is of similar size. A small difference between the two methods is only found for the total symmetric anti conformer **V**. Therefore, in the following we continue with only one functional, B3LYP. For B3LYP an increase of the basis set from 6-31+G(d) to 6-311+G(d) slightly favors the gauche conformers presumably because the closer electron distance allowing stronger intersite electron correlation. (Note that upon increase of basis set the BSSE error shifts in the other direction.)

Conformer structures of large, flexible molecules can have very different vibrational frequencies. This affects the zero-point vibrational energy and the density of thermally accessible states of the conformers. For PENNA the inclusion of the zero-point energy (ZP) changes somewhat the relative energies but not the energetic order of the conformers (Table 1). If different molecular conformer have different frequencies, the question arises whether the global minimum in the electronic potential energy landscape is also the global minimum in the free energy landscape at the nozzle temperature (~360 K).

In general, close above room temperature the influence of entropy (caused mostly by the vibrational state density) has to be discussed. To see the effect of state density the structure of the global minimum was also searched at the free energy surface. The Gibbs energy $G°$ for PENNA was determined at 298.15 K and at 360 K from the knowledge of energy, enthalpy, and entropy values as determined from *ab initio* characteristics (geometries, energies, and vibrational frequencies). In these calculations rigid rotor, harmonic oscillator and ideal gas

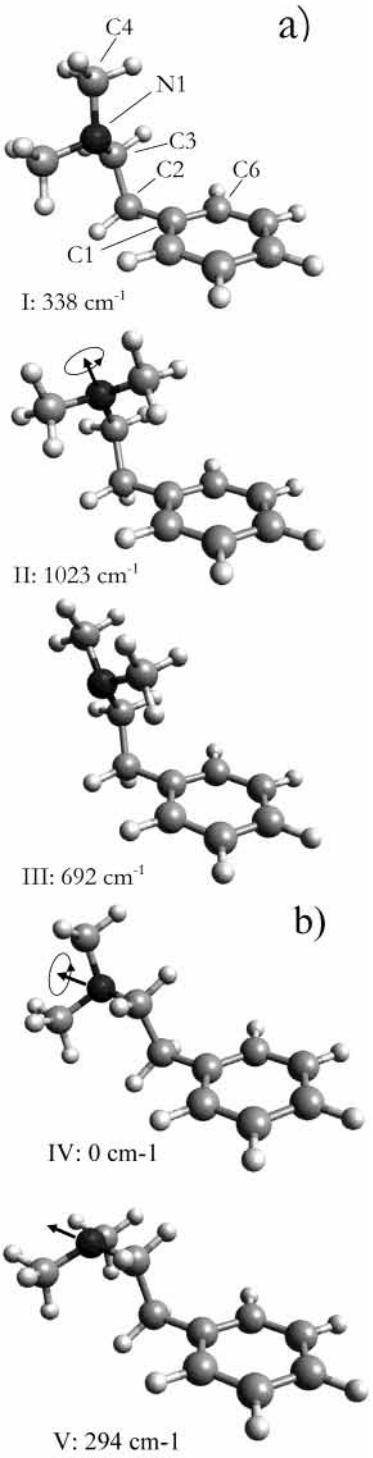

Figure 2. Structures and relative energies of neutral PENNA calculated with the B3LYP/6-31+G(d) method. (a) the gauche conformers (2-fold degenerate) and (b) the anti conformers (rotation along the C3−C2 axis). Within the families of gauche and anti structures further structural varieties are formed by rotation of the methylated amine group (rotation about the N1−C3 axis). (a) In conformer **I** the interaction of the "lone pair" orbital of N with the π system is slightly repulsive, leading to a high relative energy for this conformer. Presumably due to steric hindrances between the CH_3 groups and the π system, the conformers **II** and **III** are unfavorable in energy and not expected to be thermally populated. (b) The most stable conformer structure of PENNA is the linear asymmetric anti conformer **IV** (2-fold degenerate). Note that the symmetric anti conformer is not degenerate. The relative conformer energies with different methods and basis sets are presented in Tables 1 and 2 and the most important isomerization barriers in Figure 3. The conformer numbering corresponds to the nomenclature used previously for PEA.[13]

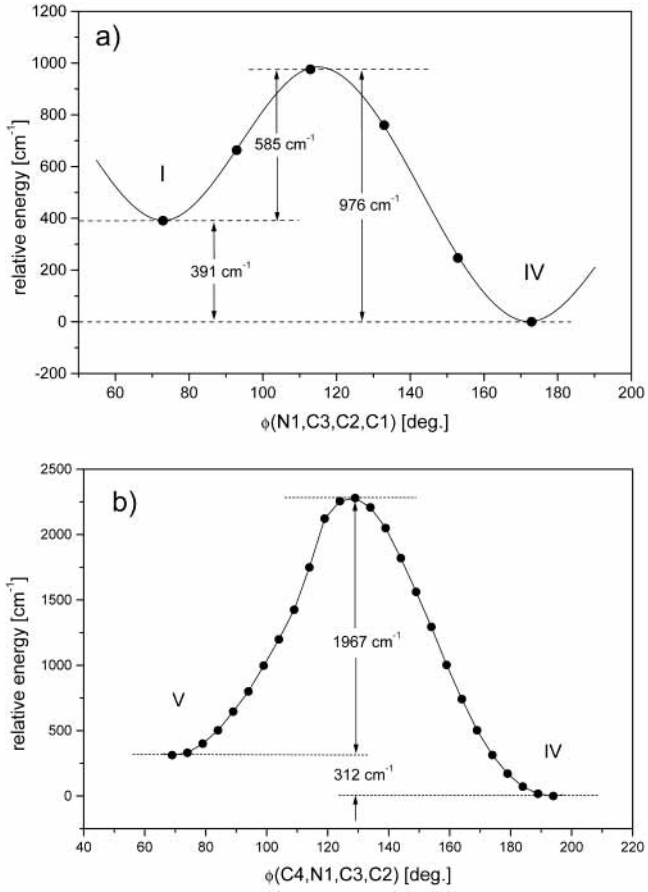

Figure 3. The two most important isomerization barriers in neutral PENNA. The isomerization paths of conformers **II** and **III** to the most stable conformer **IV** have been not investigated because of their relative high energy in comparison to conformer **IV** and the resulting low thermal population. The electronic ground-state energy is plotted in dependence of the isomerization coordinates (here dihedrical angles, for atomic labeling see Figure 2a). Energies along the isomerization paths (a) from the gauche conformer **I** to the anti conformer **IV** (here the final structure is the mirror image of the structure in Figure 2b, conformer **IV**) and (b) from the anti conformer **V** to the anti conformer **IV**. Because isomerization barriers are 585 and 1967 cm^{-1}, respectively, at 360 K conformational changes are expected to be slow in PENNA and not to take place efficiently during the supersonic expansion. For further explanation see section V.3.

approximations were adopted, although we are well aware that anharmonicity may be important. The results (see Table 1) show a stronger relative stabilization of conformer **I**, but no severe total effect: Still for both temperatures the nonsymmetric anti conformer **IV** is the most stable structure.

Due to the fact that for the discussion of conformer stability we only can rely on the R2PI intensities we are not able to perfectly weight the different theoretical levels and methods (see section V.3). An important question in this context is, how the conformer population is changed by the supersonic expansion. To obtain further understanding for the isomerization processes in PENNA, the isomerization energies for turning conformer **I** into the most stable conformer **IV** (Figure 3a) and conformer **V** into conformer **IV** (Figure 3 b) was calculated with the B3LYP/6-31+G(d) method. The energy barrier for conformational changes from the higher to the lower conformer are 585 and 1967 cm^{-1}, respectively. As will be discussed in section V.3, these barriers should be high enough that during the supersonic expansion isomerization between gauche and anti conformer classes and conformers **V** and **IV** is improbable.

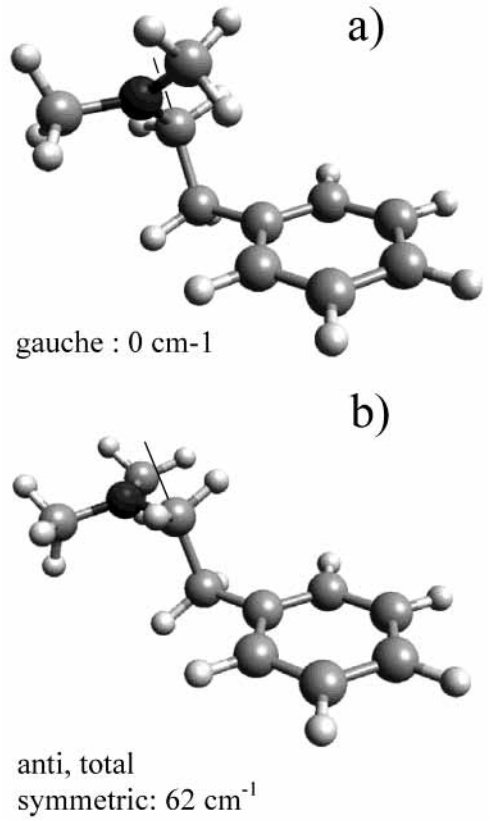

Figure 4. (a and b) structures and relative energies of the two radical cation conformers of PENNA calculated with B3LYP/6-31+G(d). Note that the amine group is mostly planar as expected in the presence of the positive charge. As a result, in the cation the number of rotamers for the gauche and the anti positions is reduced from 3 (neutral) to 1 (cation), resulting in total in only two conformers. Energies and charge and spin distribution of the ionic conformers are included in Table 3.

IV.2. Calculations of the PENNA Cation. The motivations for theoretical calculations of PENNA cations are (i) the investigation of the cation structures and (ii) the investigation of the cation ground-state charge and spin distributions. The cation structure after ionization is needed to distinguish the type ("through bond" and "through space") and the charge and spin densities for the strength of the coupling of the two sites in PENNA.

Note that in photoionization experiments the Franck Condon principle does not allow geometry changes during ionization. Hence the type of the cation conformer structure formed by ionization is given by the type of the neutral conformer structure we start with. Clearly the cation conformer should have a slightly different structure than the initial neutral conformer. In extreme cases, however, the cation structure as formed by ionization could be unstable and isomerize to a completely different structure. To clarify this, we therefore used the neutral conformer structures as a start geometry for the calculation of the cation. Because PENNA radical cations are open-shell species and computations therefore become time-consuming, only B3LYP/6-31+G(d), PW91/6-31G(d), and single-point MP2/6-31+G(d) calculations have been performed. By searching the gauche and anti subsurface of the potential surface, only one gauche and one anti conformer were found to be stable. The B3LYP/6-31+G(d) cation structures are presented in Figure 4. For all conformers the amine group becomes planar as expected in the presence of the charge. This planarity reduces the possible orientations with respect to the CH_2-CH_2 bridge (anti conformers) or the π system (gauche conformer). The corresponding relative energies are given in Table 3.

TABLE 3: Calculations of the Relative Energies as Well as Charge and Spin Densities of the Two Stable Conformers of PENNA Cations Using the B3LYP/6-31+G(d) and the PW91/6-31+G(d) Density Functional Methods[a]

		conformer	
method		gauche	symmetric anti
B3LYP/6-31+G(d)	relative energy	0	62
	partial charge in ring	10%	30%
	partial charge in tail	90%	70%
	unpaired spin in ring	15%	21%
	unpaired spin in tail	85%	79%
PW91/6-31+G(d)	relative energy	0	190
	partial charge in ring	11%	27%
	partial charge in tail	89%	73%
	unpaired spin in ring	14%	19%
	unpaired spin in tail	86%	81%
MP2/6-31+G(d)[b]	relative energy	0	1019
	partial charge in ring	8%	18%
	partial charge in tail	92%	82%
	unpaired spin in ring	2.6%	3%
	unpaired spin in tail	97.4%	97%

[a] The B3LYP conformer structures of the cation ground state are presented in Figure 4. Note that in the cation the order of stability between gauche and anti is reversed in comparison to the neutral molecule. Nevertheless there is an anti conformer which is a stable cation structure. To compare the charge densities calculated with B3LYP and PW91, single-point MP2 calculations have been performed also. All methods agree that in the cation ground state for both conformers most of the charge is concentrated on the amine site. This is also in agreement with a planar amine structure (Figure 4) which reduces the number of rotamers. In the most predominant extended symmetric anti conformer of PENNA, there is still considerable charge delocalization into the phenyl ring for B3LYP (30%) and MP2 (18%) calculations. Note that this delocalization might be caused by polarizability rather than by coupling. To obtain more evidence for this, spin densities have been calculated for the B3LYP and MP2 results. Only the MP2 calculations strongly localize the unpaired spin at the amine group. Although a weighting of the methods concerning their accuracy is difficult, our result of a weak intersite laser ionization favors the MP2 spin density result. In conclusion the calculations support the assumption of mostly local electronic states for the first two electronic states of PENNA cations and are in agreement with the interpretation of previous He I PE spectra[10] (for further explanations see text). All energies are given in cm^{-1}. [b] Single-point calculation with the B3LYP 6-31+G(d) geometry.

With respect to the HeI spectra,[10] the most interesting question is whether the cation ground state has a preferential charge localization at the amine group. Intramolecular charge distributions were calculated from Mulliken charges[30] (Table 3). For this for each atom the difference in charge between the neutral and the radical cation was calculated. For the two cation conformers all calculation methods agree that most of the surplus positive charge is on the amine group (Table 3). The calculated charge delocalization from the amine group into the ring is relatively strong (B3LYP, 30%; PW91, 27%; and MP2, 18%.). The fact that the gauche conformer becomes energetically slightly more stable than the trans conformer may be due to solvation of the charge by the benzyl group (see Table 3).

As explained in section V.5 we find some discrepancy between the relatively large charge delocalization and the observed high site-selectivity of ionization. If the charge delocalization in the cation ground state of the anti conformer is taken as a criterion for the coupling of the two sites we expect some nonvanishing intersite ionization. The fact that this is not found (section V.5) rises the question whether the charge and the intersite coupling are directly correlated or not. An argument that the charge density might not directly correspond to the intersite coupling is that electron delocalization in the presence of an electron hole affects all electrons of all orbitals, but the

intersite coupling is predominantly an interaction of the higher MOs of the two sites. The spatial electron shifts in lower orbitals which were induced by the coulomb force of the positive charge can be best described as a static polarization. Such static polarization of electrons in lower MOs is not expected to strongly influence the intersite coupling.

To eliminate the polarization we analyze the localization of the electron hole, i.e., the localization of the spin density of the unpaired electron. Because the polarization equally affects electrons of up and down spin, the spin density does not contain contributions of the electron shifting in lower MOs caused by the positive charge. To check this we performed spin density calculations with the B3LYP and MP2 (single-point) methods. Spin and charge densities are comparable for B3LYP but different for MP2 (Table 3). The 3% spin density in the ring calculated for the PENNA cation ground state would much better correlate with the high spatial selectivity of the ionization process. Unfortunately for radical ions there is so far no experience concerning the accuracy of calculated charge and spin densities. Our results (section V.5) support that the spin delocalization calculated by MP2 might be more accurate for the description of the coupling of the first two cation states than the charge delocalization.

From the fact that the lowest cation state is due to preferential charge and spin localization at the amine, we expect that the second electronic state in the HeI PE spectrum[10] which lies about 0.7 eV above the cation ground state is a state with a preferential charge localization at the aromatic chromophore. Calculations for this electronic excited state, however, would have to be performed at the CASPT2 level. Because of the large number of heavy atoms in PENNA, so far such calculations are impossible.

In conclusion, all levels and methods of theory used predict that the linear anti structure is by far the most stable conformer in neutral PENNA and that the cation ground state has a predominant charge distribution at the amine group.

V. Experimental Results and Discussion

In the following we describe the experimental setup (section V.1), present R2PI spectra (section V.2), compare these experimental results with theoretical calculations (section V.3), and present R2PI mass spectra (section V.4) and results of two-photon two-color laser experiments (section V.5).

V.1. The Experimental Setup. The experimental setup for the R2PI reflectron time-of-flight mass spectrometer (RETOF-MS) is described elsewhere.[3,4,35−37] In short the reflectron RETOF-MS consists of a supersonic jet chamber, an ion source chamber, a field-free drift region, a two-stage reflectron, a multichannel plate detector, and a digital oscilloscope. A pulsed nozzle (General Valve, orifice diameter 300 μm) is heated to 360 K to achieve a suitable sample vapor pressure of PENNA. We especially reduced sample water impurities by molecular sieve. A mixture of about 3% (estimated maximum value) of sample molecules in Ar rare gas was expanded in a pulsed supersonic expansion (Ar backing pressure: 5 bar). 100 mm downstream of the nozzle PENNA ions were formed by one-color R2PI in a two-stage ion source. The ions were accelerated (final ion energy: 1600 eV) and mass-separated by time-of-flight in a RETOF-MS. The ion reflector was used for flight-time compensation due to the initial molecular velocities and the finite size of the laser focus.[35−37] Detuning of the reflector voltages allows detection of fragment ions which have been formed by metastable decay in the drift region.[34] In the correction mode the mass resolution of the RETOF was above $m/\Delta m = 3000$ for masses above 100 Dalton. The S_0-S_1 R2PI spectrum of PENNA was recorded by detection of the parent and the amine fragment cation intensities. Both R2PI spectra contain essentially the same features. Because of the strong fragmentation, the spectrum recorded by parent cation detection is noisy and therefore not shown here.

Laser excitation was performed by the second harmonics of an excimer-pumped dye laser (5−7 ns pulse width, 10−100 μJ UV pulse energy, focused down to a 1 mm diameter, wavelength range: 250−270 nm). To test intersite ionization two time-synchronized laser pulses of different colors overlapping in space were used. In resonant two-photon two-color ionization experiments (R(1+1')PI) laser 1 was set to the S_0-S_1 origin transition and laser 2 tuned to different discrete UV wavelengths. A short delay of 5 ns of laser 2 versus laser 1 was used to test if ionization from the S_1 in the phenyl group to the amine group is possible (intersite excitation). The UV photon energies were red-shifted against laser 1 (nonresonant with the S_0-S_1 transition) and the intensity of laser 1 was attenuated to reduce the one-color contribution to the ion signal. The technique for metastable decay measurements is described in ref 35.

V.2. The Resonant Two-photon Photoionization (R2PI) Spectrum of PENNA. While recording the R2PI spectrum of PENNA, we observed very strong fragmentation even at a low laser intensity of 2×10^5 W/cm^{-2}. In Figure 5 we present the corresponding R2PI mass spectra of PEA (a) and PENNA (b). Both mass spectra were recorded at the same UV laser intensity. Whereas for PEA no fragmentation is observed, for PENNA the parent-to-fragment ion intensity ratio is about 1:10. This demonstrates that for PEA a fragment-free ionization is possible, but not for PENNA. The strong fragmentation seems to be a special property of PENNA. The possible reasons are discussed in section V.4.

Because of the strong fragmentation, the one-color S_0-S_1 R2PI spectrum of PENNA (Figure 6) was recorded by detection of the ion current of the intense amine fragment, the immonium ion of mass 58 Da. Although we detected the daughter mass, we present evidence that this spectrum is the S_0-S_1 spectrum of intact PENNA. The evidences are as following:

(i) The R2PI spectrum taken via the parent cation mass (not shown here) has essentially the same spectral features, but just a smaller signal-to-noise ratio.

(ii) The R2PI spectrum lies at the typical transition energy expected for a substituted benzene (S_0-S_1 origin: 37608 cm^{-1}).

(iii) The peak pattern in the R2PI spectrum is similar to the vibrational pattern of the benzene S_0-S_1 spectrum.

(ii) For comparison of peak positions the R2PI spectrum of PEA is presented in the left upper corner of Figure 6. The agreement of the transition energy of PENNA with that of the conformers of PEA is good: They all lie in a 100 cm^{-1} range which is a confirmation of the local concept for the neutral molecules. Different conformer structures and even the size of the molecule do not severely influence the chromophore. In PEA four nearly equally stable conformers exist which have been assigned to two gauche and two anti conformers.[7,13,32,33] The interpretation of the conformer intensities is difficult and discussed it in a separate subsection (V.3).

(iii) The R2PI spectrum of PENNA is sharp as expected for a long-lived phenyl S_1 state. We find no indication of fast S_1 dynamics. The spectrum carries the vibrational fingerprint of the aromatic phenyl chromophore (vibronic transitions $6b_0^1$, 12_0^1, and $18a_0^1$, see assignments in Figure 6). If one compares the data of PENNA and ethylbenzene (EBZ)[24] the agreement is nearly perfect: $6b_0^1$ in PENNA = 529 cm^{-1} versus that in

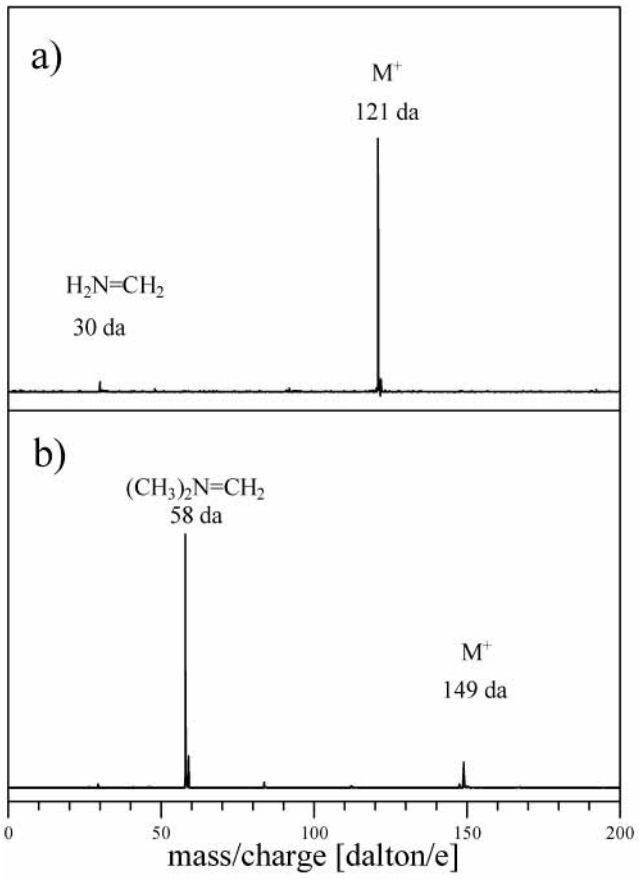

Figure 5. R2PI mass spectra (raw data) of (a) PEA and (b) PENNA taken via origin transitions and at low laser intensity ($I \sim 2 \times 10^5$ W/cm^2). The absolute total ion current per laser shot in both cases is about the same ($N \sim 500$ ions per laser shot, mass spectrum averaged over 50 shots). (a) At this low laser intensity, PEA can be ionized and detected as intact molecules. Only small traces of immonium fragment cations of mass 30 dalton are found. Because of the low dissociation energy in amine compounds, this experiment clearly shows that cation UV photoabsorption can be fully avoided at such low laser intensity. At high laser intensity ($I \sim 10^8$ W/cm^{-2}, not shown here) cation UV photoabsorption takes place and strong, prompt dissociation is observed in PEA. (b) At the same low laser intensity used in a) strong fragmentation takes place for PENNA. This behavior of PENNA is rather unexpected because the example of PEA in (a) shows that in the same chromophore cation UV photoabsorption can be avoided. With the help of the RETOF-MS one can show that the cation decay of PENNA is metastable (decay rate $\sim 5-10\ \mu$s) and therefore not caused by cation UV photoabsorption. The only explanation we see is that fragmentation happens directly after ionization (for further explanation see text).

EBZ = 529 cm^{-1}; 12_0^1 in PENNA = 930 cm^{-1} versus that in EBZ = 931 cm^{-1}; and $18a_0^1$ in PENNA = 969 cm^{-1} versus that in EBZ = 969 cm^{-1}. One of the small transitions (d) at relatively low energy is presumably attributed to a tail-to-chromophore mode (PENNA = 326 cm^{-1}, in EBZ = 344 cm^{-1}[24]). This agreement of vibrational features with a benzene derivative and the agreement of absolute energy position leaves no doubt of an excitation at the phenyl chromophore.

In total arguments (i) to (iii) leave no doubt that the spectrum in Figure 6 is the R2PI spectrum of the intact PENNA molecule. Close to the most prominent origin transition some small peaks are observed which could be due to Ar clusters (note that the cluster would fragment see subsection V.4) or other conformers. The conformer intensities are discussed in the next subsection.

V.3. Discussion of the Conformer Intensities in the R2PI Spectrum. The interpretation of the conformer intensity of the

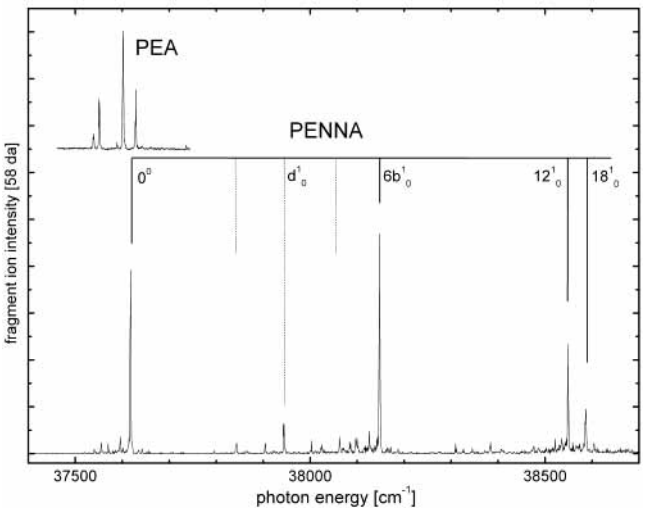

Figure 6. R2PI spectrum of the S_0-S_1 transition of PENNA monitored by the immonium fragment cation of mass 58 dalton. The absolute position (S_0-S_1 origin transition at 37608 cm^{-1}) as well as the presence of benzene vibrations clearly proves the excitation and ionization via the S_1 state of the aromatic chromophore and hence the assignment to the intact species. The spectrum recorded by the parent mass (not shown here) is noisy but essentially contains the same transitions. In agreement with theoretical predictions (Table 1) one conformer is predominant and with high confidence attributed to the asymmetric anti conformer (conformer **IV**). The inset in the upper left corner shows the origin region of the R2PI spectrum of the unsubstituted species PEA with its four conformer origins (drawn to the same energy scale) for comparison. Note the small shift between the origins of PEA and PENNA clearly indicating that the R2PI spectrum, although recorded by amine fragment ion intensity detection, is the spectrum of the intact PENNA molecule. For further explanation see text.

R2PI spectrum is not an argument for the key message of this work. Nevertheless we here indulge somewhat in providing arguments why we believe that for PENNA the initial conformer population in the supersonic expansion is mostly conserved during the supersonic expansion.

The use of supersonic molecular beams to prepare internally very cold, gas-phase samples has become well established.[38,39] From this usually one would expect that only the most stable conformer can be found after supersonic expansion. In practice, however, the interpretation of the conformer intensities in the R2PI spectrum of PENNA is difficult. If one assumes similar optical transition moments for all conformers their intensities in the R2PI spectrum should somehow reflect the relative population of the conformers at the time and site of ionization. To exclude the effect of different R2PI cross sections of the conformers, spectra with different laser intensities were recorded (not shown here). They contained no remarkable intensity changes between the most prominent origin peak and the close-by small peaks which are attributed to other conformers.

The conformer population at the time of ionization very strongly depends on the initial gas phase conformer distribution in the nozzle directly after evaporation, its equilibration in the nozzle and its transformation by the supersonic beam. Clearly thermal and collisional energies, isomerization barrier heights and the time interval are the relevant parameters.

The best argument that the initial conformer of PENNA is conserved in the supersonic beam are the barriers for iosmerization. As mentioned in section IV.3 the calculated barriers for isomerization from conformer **I** to conformer **IV** and from conformer **V** to **IV** are 585 and 1967 cm^{-1} respectively. These values are clearly considerably higher than the energy of thermal

collisions at the nozzle temperature of 360 K ($E_{trans} \cong 242$ cm^{-1}). Isomerization barriers from conformers **II** and **III** to conformers IV were not calculated, because conformers **II** and **III** lie at such high energies that they are extremely weakly populated at 360 K.

Investigations of Ruoff et al. for flexible molecules in He, Ne, Ar, Kr, and Xe expansions showed[42] that high-energetic conformers do not isomerize in the supersonic expansion if the barrier is higher than 350 cm^{-1}. Our barrier values are considerably above 350 cm^{-1}, and therefore, we can assume that the conformer population as present in the nozzle at 360 K is mostly preserved in the supersonic expansion. Clearly due to the broad thermal distribution of internal energy at 360 K, some molecules might have always enough energy to be above the barrier. The percentage of molecules with such a high a energy is, however, small. An other effect might be a structural change by transient cluster formation. Because the binding energies of Ar to molecules is relatively small[42] this effect also clearly can only become important for molecules with low isomerization barriers.

The molecules investigated by Ruoff at al. were, however, relatively small.[42] Note that PENNA is already a fairly large molecule, has 72 normal modes and especially a lot of low-frequency modes, i.e., a high density of states at the energy of the barrier. So thinking of isomerization as a statistical process, considerable energy over the isomerization barrier is needed for an isomerization on a μs time scale. Whereas the residence time of an evaporated molecule in the gas phase in the nozzle is long [longer than 50 ms (repetition rate of 20 Hz)], the cooling time in supersonic expansions is very fast.[38−44] For vibrations the fastest cooling occurs in or just behind the nozzle and then quickly saturates with distance, corresponding to a cooling time of some microseconds. This short cooling time also supports conservation of conformer population during expansion.

Usually for stiff molecules the vibrational cooling is not very efficient. For flexible molecules with low-frequency modes an extraordinary efficient cooling of internal degrees of freedom was found.[43,44] This is explained by IVR to the low-frequency modes and an efficient coupling of the low-frequency modes to the translational degrees of freedom of the carrier gas expansion. This efficient vibrational cooling for flexible molecules supports a conservation of the conformer structure during expansion.

In total we have good arguments to assume that the conformer population of PENNBA as present in the nozzle at 360 K is mostly conserved in the supersonic expansion.

We now roughly interpret the intensities under the above assumption of full conformer conservation in the supersonic jet. A detailed analysis of the conformer intensities nevertheless might be difficult, because of the entropy effect which is difficult to calculate due to anharmonicity. In contrast to PEA, PENNA has only one predominantly stable conformer. Some small structures to the left side of the strong origin are tentatively attributed to other conformers or fragmented clusters. The intensity ratio of the other possible conformers to the most stable conformer is about 1/10. This means that the thermal population of these conformers at 360 K is low. With the exception of the symmetric anti conformer all conformers of PENNA are doubly degenerate. Estimated from the intensities in the R2PI spectrum the energy differences of the less stable conformers to the most stable conformer should be equal or larger than 242 cm^{-1} (kT at 360 K). This is qualitatively in good agreement with the B3LYP and PW91, but not well with the MP2 calculations, which predicts two similar intense conformers (section IV.1). Nevertheless for a comparison between theory and experiment one also has to keep in mind that the calculated absolute energies are great and the relative conformer energies very small. Due to the small basis sets used and/or error compensation, a more inaccurate method may accidentally provide better relative energies than the theoretically more exact method. All theoretical levels and methods, however, agree on conformer **IV** to be the most stable and we therefore attribute the observed predominant bands to the R2PI spectrum of structure **IV**. This prediction of the neutral structure of PENNA has been our main motivation for these calculations.

V.4. Mass Spectra and Detection of the Metastable Character of the Decay. So far no explanation is given for the strong R2PI fragmentation in PENNA (Figure 5b). We consider the following explanations (i) thermal decomposition before laser excitation and ionization of the amine fragment, (ii) dissociation in S_1 and subsequent photoionization of the amine fragment, and (iii) dissociation after cation photoabsorption or (iv) dissociation directly after ionization. In the following we rule out possibilities (i), (ii), and (iii).

(i) We have no indication of a neutral dissociation at the temperatures used, even at very long heating times. A neutral fragmentation and a subsequent ionization of the neutral amine fragment would only be possible if the laser wavelength is resonant with an excited state of the neutral amine fragment. The amine resonances, however, lie at shorter wavelengths than the laser wavelength used and in addition its photoabsorption cross section is much lower in comparison to the phenyl chromophore. These considerations are not consistent with the strong total ion signal of PENNA and its fragment, which is similar to the ion signal of PEA. Also the vibrational pattern of the R2PI spectra agrees with the benzyl chromophore, but not with amine chromophore vibrations. Thus dissociation prior to laser excitation is ruled out.

(ii) The same arguments as in (i) also hold for a fast dissociation in the neutral excited state and a subsequent ionization of the neutral amine ground state fragment. An additional argument is that the total process would be a three-photon process and therefore weak. Formation of an electronically excited amine fragment in neutral dissociation of PENNA is energetically ruled out. Proton transfer at the S_1 energy is also impossible due to the large coulomb energy needed to separate the opposite charges. H atom transfer after ionization should lead to mass 59 Da. All these arguments rule out possibility (ii). An additional argument will be provided in a forthcoming paper where femtosecond (fs) laser pulses were used for R2PI of PENNA. Because of the sharp structures in the ns R2PI spectrum the estimated minimum lifetime of PENNA in S_1 is longer than 100 ps. If there would be a dissociation on this time scale, femtosecond laser pulses could overcome such a slow rate and the parent-to-fragment ion ratio should increase considerably. This is, however, in contrast to our observation. In conclusion a neutral S_1 dissociation can be excluded.

(iii) In Figure 5 the R2PI mass spectra of PEA (a) and PENNA (b) are displayed for comparison. For PEA the S_0-S_1 origin of the most intense conformer was chosen, but the R2PI mass spectra of the other conformers are essentially the same. At the low laser intensity of about 2×10^5 W/cm^{-2} (10 μJ/pulse per 1 mm^2) in PEA only very weak fragmentation is observed (soft ionization[36]). This proves that at the low intensities used UV photoabsorption of the cation does not occur. In a state where the charge would be in the phenyl chromophore the absorption cross sections of PEA and PENNA cations should

be comparable. If the charge were in the amine site for PENNA, a lower transition moment is expected than for PEA with the charge in the phenly group. Because at the low laser intensities used PEA does not fragment and hence does not absorb UV light, the similar or smaller transition moments for UV photoexcitation in PENNA should result in no photoexcitation and hence in no photofragmentation. Despite the low laser intensity, only few intact PENNA parent cations survive in the RETOF mass spectrometer (Figure 5b), indicating that there exists another reason for the strong fragmentation in PENNA after ionization. To explain the fragment intensity difference of PEA and PENNA exclusively by cation UV absorption, for PENNA the photoabsorption cross section must be a factor of 100 higher than for PEA. This is highly improbable, and therefore possibility (iii) is with high confidence ruled out.

(iv) To confirm that possibility (iv) is responsible for the fragmentation of PENNA. we conducted further investigations. If the dissociation of PENNA takes place directly after ionization the maximum excess energy in the ion could be about 1.5 eV ($2h\nu - IE_{amine}$ with $2h\nu = 9.326$ eV and $IE_{amine} \sim 7.8$ eV). At such low energies in such a large molecule, a metastable decay is expected for fragmentation via a barrier. Indeed such a delayed decay was found by mismatching the correction conditions of the reflector of the RETOF. To get a rough estimate of the percentage of the molecules which decay in the ion source and in the field-free drift region, the reflector voltage was reduced by the factor of the fragment-to-parent mass ratio 58/149 to allow full energy correction for the immonium fragment ions formed in the first pass of the drift region (for an explanation of this technique, see ref 35). From this we distinguish between ion decay in the ion source and in the first field-free drift region. This intensity ratio allows an estimate of the decay time. A decay time of 5−10 μs was estimated for the decay of PENNA to the immonium fragment. Because of the broad distribution of internal energies in the molecular ensemble, one cannot expect to obtain a single-exponential decay even for a statistical dissociation. Therefore, we did not indulge in these decay time measurements. A rough estimation, however, shows that, because of the short drift time (20 μs) in the first field-free region of our RETOF-MS, ions which are detected at the mass of the parent ion might be already fragment ions: If the parent ions decay in the field-free drift tube after the reflector the resulting fragment ions are detected at the flight time of the parent cation mass.

Photofragmentation of PEA cations ($h\nu_{UV} \sim 4.663$ eV) was measured to be faster than 100 ns (not shown here). The slow metastable 5−10 μs decay of PENNA cations is therefore an additional indication that fragmentation in the cation is not caused by UV photoabsorption.

As mentioned above, directly after ionization the maximum excess energy in PENNA ions is 1.5 eV. As is well-known for large molecules, the statistical dissociation is slowed because of the large number of degree of freedoms and the resulting high density of vibrational states on which the energy can be efficiently distributed.[45] Despite this relatively small excess energy and the relatively large size of PENNA, the decay is in the short microsecond time regime. This can be only understood by a small dissociation energy.[45] In our former work on small peptides we estimated from the heat of formation tables that about 0.5 eV vibrational energy above the local IE of the amine group is necessary to observe cation dissociation at this site.[3] Because of the similarity of the **N** terminal in peptides and the amine group, the local threshold for fragmentation in PENNA is expected to be of similar size. Due to the kinetic shift effect surely the dissociation energy is smaller than the energy where fragmentation is observed in our RETOF.

Usually in ionization the leaving electron takes most of the photon excess energy away. The remaining question is then which mechanism provides enough energy for mostly all and not just a few PENNA cations to cause such efficient fragmentation. We believe that we have gathered strong arguments that this mechanism is the local ionization in the phenyl chromophore to the second electronic state of the PENNA cation and a subsequent charge transfer to the lower-energetic amine site. In principle the time until fragmentation is observed is composed of the charge transfer and the fragmentation time. Because CT in the cation is expected to be fast,[17] the fragmentation is the rate determining step. Its metastable character of the fragmentation then clearly shows that fragmentation has a nonvanishing dissociation barrier.

V.5. Exclusion of Intersite Ionization to the Amine Cation State: Two-Photon Two-Color Laser Experiments. In this subsection we first discuss the hypothetical influence of a intersite ionization on the fragment pattern of the R2PI mass spectrum and then report on a two-color R(1+1')PI laser experiment which directly checks whether an intersite excitation is possible.

Calculations of the cation ground state predict a considerable charge delocalization into the phenyl ring indicating some coupling between the two sites. Therefore in principle we cannot exclude that via the S_1 of the phenyl group some molecules can be ionized directly at the amine site. For the following we assume that such an intersite photoionization to the ion ground state with the charge at the amine group is possible. Then the observed strong fragmentation directly after ionization needs an explanation. For fragmentation to occur at least 0.5 eV internal energy in the cation are necessary (see section V.4). This is, however, very untypical for a R2PI process: Usually the electron takes most of the excess energy away as kinetic energy. Even if the Franck−Condon factors favor high vibrational excitation, as expected for ionization of an amine group, this does not explain a high-vibrational excitation of the vast majority of the PENNA molecules. Still, a considerable amount of molecules should be left with less than 0.5 eV vibrational excess energy and stay stable as intact parent molecules. This is, however, not observed.

To provide further experimental evidence that two-photon intersite ionization is weak or impossible, also a two-color two-photon ionization was performed. The first laser (laser 1) was set to a S_0-S_1 resonance of PENNA and the wavelength of the second laser (laser 2) was tuned. The ionization onset was so soft and broad that it was impossible for us to record an ionization spectrum with reasonable stability and signal-to-noise ratio. To decide which electronic state of the cation is excited in the ionization process, however, experiments with laser wavelengths of laser 2 in two ranges are sufficient, above and below the expected ionization energy of the second electronic state of the cation ($IE_{phenyl} = 8.5$ eV, ionization to the phenyl site). First wavelengths of laser 2 were chosen to have total photon energies ($h\nu_1 + h\nu_2$) above the IE of the phenyl site (8.6 and 8.8 eV). In this experiment a strong two-photon ion signal was observed. The ionization cross section was found to be by about a factor of 2 larger for the 8.8 eV excitation than for 8.6 eV total photon energy. For total photon energies below the expected IE of the substituted phenyl ring ionization at this site becomes impossible, but still ionization to the amine site is energetically possible ($IE_{amine} = 7.8$ eV).

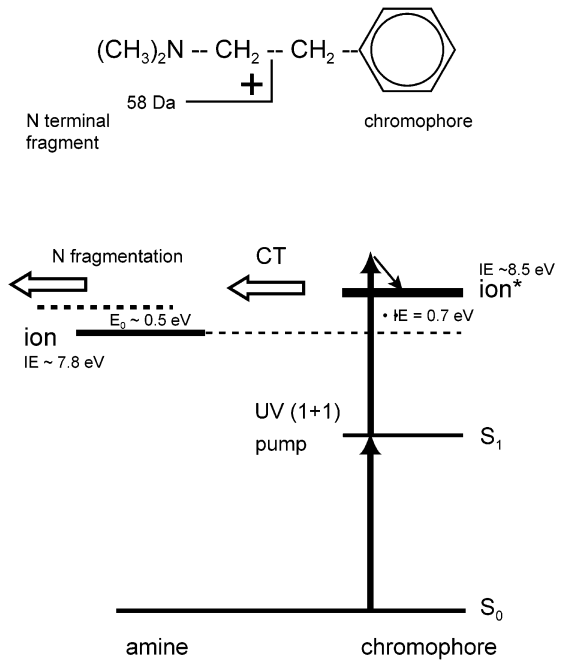

Figure 7. Explanation of the fragmentation of PENNA directly after ionization: After local ionization of the benzyl chromophore (first excited electronic state of the cation) the positive charge is transferred to the lower energetic amine site (cation ground state). In this process the electronic excess energy is converted to vibrational energy leading to metastable dissociation at the amine site. The excess energy set free in this process is about 0.7 eV. Efficient dissociation is expected 0.5 eV above the local IE at the amine group. The fragmentation is metastable, in good agreement with the large size of PENNA and the relatively low excess energy. Due to our limited detection time window for metastable fragmentation, one can assume that even most of the rest of the ions detected in our mass spectrometer as parent ions might have had enough internal energy to fragment outside our detection time window.

Within the experimental error at total photon energies below 8.5 eV, no two-color two-photon ion signal (neither parent cation nor fragment ion) was observed. It should be noted that due to the background caused by the one-color ion signal there is a detection threshold for the two-color ion signal in our experiment. We estimate that the two-color two-photon ion signals at total photon energies below 8.5 eV are below 10% of the R(1+1')PI signal at 8.6 eV total photon energy. The lack of a detectable R(1+1')PI ion signal at total photon energies below 8.5 eV shows that one-photon two-electron intersite ionization from S_1 of the phenyl to the amine site is much weaker than the local ionization via the phenyl chromophore.

In total we have good arguments to assign the strong fragmentation in the R2PI spectra to the very special situation in PENNA that the dissociation energy of the amine group is below the IE of the phenyl group and ionization is local at the phenyl site.

VI. Final Discussion and Conclusion

In summary the metastable decay of PENNA ions after R2PI via the S_1 of the phenyl chromophore is interpreted to be a direct signature of the local ionization at the phenyl site and a subsequent charge transfer. The full picture of the processes is presented in Figure 7. By R2PI via S_1 of the phenyl chromophore selectively local ionization to the cation first excited state at the phenyl takes place. This state is in good approximation local. By this ionization an excess energy of more than 0.7 eV is transferred to all molecules. By CT this electronic energy is converted into vibrations leading to dissociation at the amine group by formation of the immonium fragment ion with mass 58 Da (see Figure 7, molecular formula). No charged phenyl fragment is observed in the R2PI mass spectrum.

The fact that more than 90% of the PENNA molecules fragment shows that the selection rule for local ionization is rather strict. For the 10% of ions which were detected as intact PENNA ions, it can be assumed that even they contain enough energy for a decay, but outside our time window of metastable decay detection, here 20 μs. By resonant two-color two-photon ionization with different total photon energies, it was possible to provide an additional proof that ionization via S_1 in the phenyl chromophore populates the first excited state of the PENNA cation with a very high selectivity. As a consequence for PENNA the one-photon two-electron intersite excitation must be very weak. The MO analysis of the intersite excitation combined with literature data[5−7,21−23] indicates that in the case of local cation states the transition intensity for a site-selective ionization is given by a one-photon one-electron selection rule.

This result additionally supports in retrospect some previous local ionization concepts for molecules.[2−4] It seems to also be transferable to other two- or multisite molecular systems with $-CH_2-CH_2-$ spacers, extended structures, and large energy splitting of the neighboring sites. Such a situation is, for example, valid for tyrosine and tryptophan amino acids in peptides.[3,4] For folded molecules or clusters, due to through-space effects, the situation might be more complex and has to be checked system by system. According to previous experiments for molecules with energetically degenerate charge sites the local R2PI ionization scheme fails even for extended conformers.[13]

One remaining question for theory is whether the cation surplus charge distribution is the right parameter to describe an intersite coupling. In analogy to the cation ground state with a delocalization of some 15−30% charge into the ring we expect also for the first excited state of PENNA that most of the positive charge is at the phenyl site, but still some 15−30% of charge might be delocalization into the amine site. If the charge distribution would directly correspond to the coupling of the two sites, one would expect an equivalent bifurcation of the ionization to the amine and the phenyl group. In our two-photon two-color experiments no ionization via S_1 of the phenyl chromophore to the amine group was observed. This result might be an indication that the coupling between the two first electronic sates of the PENNA cation is small, especially below the percentage of calculated charge delocalization. The explanation for this difference might be that in extended cations partial charge is shifted which is not directly involved in the intersite coupling of the two electronic states. Such "inactive partial charge delocalization" is due to a shift of electrons which are in low-lying orbitals and not involved in the coupling of the two lowest local electronic states in PENNA. Interestingly this charge shift by polarization is expected to affect up and down spin electrons similar, but not the one nonpaired electron. Hence the spin density should be able to separate coupling effects from polarization effects. Whereas B3LYP and PW91 show similar spin delocalization than charge delocalization for the cation ground state, the MP2 single-point calculation shows considerably less delocalization of the unpaired spin density than calculated for the charge. Although the accuracy of the theoretical methods concerning charges and spin densities in cations is unknown, we have the impression that spin density better describes the electronic coupling of two charge sites in an extended molecule. Clearly the question how the electronic

intersite coupling is correlated with spin or charge density needs further theoretical investigation.

With high confidence and the help of theory we can state that the conformer structure of neutral PENNA is extended. Hence, the dynamics after local ionization at the phenyl chromophore is a "through bond" CT. Due to energy conservation in the gas phase, during the CT conversion of electronic energy into vibrational energy takes place. In total more than 0.7 eV of energy is set free as vibrational energy which then can lead to efficient dissociation by formation of immonium fragment ions. We believe that the CT is fast so that the metastable character of the fragmentation can be exclusively attributed to the dissociation. This is evidence against a direct fragmentation on a dissociative surface and favors the existence of a positive dissociation energy at the amine site. This dissociation energy should be less than 0.5 eV above the IE of the amine group, to explain the relatively fast metastable dissociation. Although our data do not provide contradictions to a statistical decay, we cannot exclude that a part of the molecules can overcome the dissociation barrier in a very short time by a direct coupling of the CT channel to the dissociation channel as predicted by theory.[46,47]

Although complex, our explanations are conclusive and we believe to have good evidences that the lowest two electronic states in PENNA are mostly local and that R2PI through the phenyl S_1 state is local in the phenyl chromophore. The proof of the local ionization and the evidences for a linear structure of PENNA are essential for the forthcoming paper which reports on femtosecond CT dynamics in PENNA.[17]

Acknowledgment. R.W. thanks the *Volkswagen-Stiftung* and the *Fond der Chemischen Industrie* for financial support. A.M. thanks the *Internationales Büro des BMBF* at the DLR for travel expenses.

References and Notes

(1) Lakowicz, J. R, *Priciples of Fluorescence Spectroscopy*; Kluwer Academic Plenum Publishers: New York, 1999.

(2) Cattoraj, M.; Laursen, S. I.; Paulson, B.; Chung, D. D.; Closs, J. L.; Levy, D. H. *J. Phys. Chem*. **1992**, *96*, 8778.

(3) Weinkauf, R.; Schanen, P.; Yang, D.; Soukara, S.; Schlag, E. W. *J. Phys. Chem*. **1995**, *99*, 11255.

(4) Weinkauf, R.; Schanen, P.; Metsala, A.; Schlag, E. W.; Bürgle, M.; Kessler, H. *J. Phys. Chem*. **1996**, *100*, 18567.

(5) Dao, P. D.; Castleman A. W. *J. Chem. Phys*. **1986**, *84*, 1435.

(6) Brutschy, B. *Chem. Rev*. **1992**, *92*, 1567.

(7) Yao, J.; Im, H. S.; Foltin, M.; Bernstein, E. R. *J. Phys. Chem*. **2000**, *104*, 6197.

(8) Cannington, P. H.; Ham, N. S. *J. Electron Spectrosc. Relat. Phenom.* **1979**, *15*, 79; *J. Electron Spectrosc. Relat. Phenom*. **1983**, *32*, 79.

(9) Debis, T. P.; Rabalais, J. W. *J. Electron Spectrosc. Relat. Phenom*. **1974**, *3*, 315.

(10) Domelsmith, L. N.; Munchhausen, L. L.; Houk, K. N. *J. Am. Chem. Soc*. **1977**, *99*, 4311.

(11) Kimura, K.; Katsumata, S.; Achiba, S.; Yamazaki, T.; Iwata, S. *Handbook of HeI Photoelectron Spectra of Fundamental Organic Molecules*, Japan Scientific Press: Tokyo, 1980.

(12) Weinkauf, R.; Lehrer, F. In *Resonance Ionization Spectroscopy*; Vickerman, J. C., Lyon, I., Lockyer, N. P., Parks, J. E., Eds.; The American Institute of Physics: Bristol, 1998; p 117.

(13) Weinkauf, R.; Lehrer, F.; Schlag, E. W.; Metsala, A. *Discuss. Faraday Soc*. **2000,** *115*, 363.

(14) Ohashi, K.; Nakai, Y.; Shibata, T.; Nishi, N. *Laser Chem*. **1994**, *14*, 3.

(15) Inokuchi, Y.; Ohashi, K.; Matsumoto, M.; Nishi, N. *J. Phys. Chem.* **1995**, *99*, 3416.

(16) Ohashi, K.; Nakane, Y.; Inokuchi, Y.; Nakai, Y.; Nishi, N. *Chem. Phys.* **1998**, *239*, 429.

(17) Lehr, L.; Horneff, T.; Weinkauf, R.; Schlag, E. W. *J. Phys. Chem. A*. In preparation.

(18) McLafferty, F. W.; Tureček, F. *Interpretation of Mass Spectra*; University Science Books: Sausolito, 1993.

(19) Willey, K. F.; Cheng, P. Y.; Bishop, M. B.; Duncan, M. A. *J. Am. Chem*. Soc. **1991**, *113*, 4721.

(20) Bieske, E. J.; Silova, A. M.; Friedmann, A.; Maier, J. P. *J. Chem. Phys*. **1992**, *96*, 7535.

(21) Rabalais, J. W. *Priciples of Photoelectron Spectroscopy*; John Wiley & Sons: New York, 1974.

(22) Blanchet, V.; Zigerski, M. Z.; Seidemann, T.; Stolow, A. *Nature* **1999**, *401*, 52.

(23) Blanchet, V.; Zigerski, M. Z.; Stolow A. J. *Chem. Phys*. **2001**, *114*, 1194.

(24) Lehrer, F.; Lehr, L.; Weinkauf, R.; Schlag, E. W.; Hobza P.; Metsala, A. *J. Phys. Chem.* In preparation.

(25) Halpert, J.; Orgel, L. E. *Discuss. Faraday Soc*. **1960**, *29*, 32.

(26) McConnel, H. M. *J. Chem. Phys*. **1961**, *35*, 508.

(27) Reimers, J. R.; Hush, N. S. *Chem. Phys*. **1989**, *134*, 323.

(28) Remacle, F.; Ratner, M. A.; Levine, R. D. *Chem Phys. Lett*. **1998**, *285*, 25.

(29) Shulgin A.; Shulgin, A. *A Chemical Love Story*; Transform Press: Berkeley, 1995.

(30) Frisch, M. J.; Trucks, G. W.; Schlegel, H. B.; Scuseria, G. E.; Robb, M. A.; Chesemann, J. R.; Zakrewski, V. G.; Montgomery, J. A.; Stratmann, R. E.; Burant, J. C.; Dapprich, S.; Millam, J. M.; Daniels, A. D.; Kudin, K. N.; Strain, M. C.; Farkas, O.; Tomasi, J.; Barone, V.; Cossi, M.; Cammi, R.; Mennucci, B.; Pomelli, C.; Adamo, C.; Clifford, S.; Ochterski, J.; Petersson, G. A.; Ayala, P. Y.; Cui, Q.; Morokuma, K.; Malick, D. K.; Rabuck, A. D.; Raghavachari, K.; Foresman, J. B.; Cioslowski, J.; Oritz, J. V.; Stefanov, B. B.; Liu, G.; Liashenko, A.; Piskorz, P.; Komaromi, I.; Gomperts, R.; Martin, R. L.; Fox, D. J.; Keith, T.; Al-Laham, M. A.; Peng, C. Y.; Nanayakkara, A.; Gonzales, C.; Challacombe, M.; Gill, P. M. W.; Johnson, B. G.; Chen, W.; Wong, M. W.; Andres, J. L.; Head-Gordon, M.; Replogle, E. S.; Pople, J. A. *Gaussian 98*, revision C; Gaussian, Inc.: Pittsburgh, PA, 1998.

(31) Ponder, J. W. Programm TINKER, version 3.8; 2000 (http://dasher.wustl.edu/tinker/).

(32) Sun, S.; Bernstein, E. R. *J. Am. Chem. Soc*. **1996**, *118*, 5086.

(33) Dickinson, J. R.; Hockridge, M. R.; Kroemer, R. T.; Robertson, E. G.; Simons, J. P.; McCombie, J.; Walker, M. *J. Am. Soc*. **1998**, *120*, 2622.

(34) Hockridge, M. R.; Robertson, E. G. *J. Phys. Chem. A* **1999**, *103*, 3618.

(35) Kühlewind, H.; Boesl, U.; Weinkauf, R.; Neusser, H. J.; Schlag, E. W. *Laser Chem.* **1983**, *3*, 3.

(36) Neusser, H. J.; Boel, U.; Weinkauf, R.; Schlag, E. W. *Int. J. Mass Spectrom. Ion Proc*. **1984**, *60*, 147.

(37) Karataev, V. I.; Mamyrin, B. A. Shmikk, D. V. *Zh. Tekh. Fiz*. **1971**, 41, 1498.

(38) Kantrowitz, A.; Grey, J. *Rev. Sci. Instrum*. **1951**, *22*, 328.

(39) Smalley, R. E.; Wharton, L.; Levy, D. H. *Acc. Chem. Res.* **1977**, *10*, 139.

(40) Levy, D. H. *Science* **1981**, *214*, 263.

(41) Rizzo, T. R.; Park, Y. D.; Petenau, L.; Levy, D. H. *J. Chem. Phys.* **1985**, *83*, 4819.

(42) Ruoff, R. S.; Klots, T. D.; Emilsson, T.; Gutowsky, H. S. *J. Chem. Phys.* **1990**, *93*, 3142.

(43) Mayer, P. M.; Baer, T. *Int. J. Mass Spectrom. Ion Proc*. **1996**, *156*, 133.

(44) Mejer, G.; de Vries, M. S.; Hunziger, H. E.; Went, H. R. *Appl. Phys. B* **1990**, *51*, 395.

(45) Griffin, L. L.; McAdoo, D. J. *J. Am. Soc. Mass Spectrom*. **1993,** *4*, 11.

(46) Weinkauf, R.; Schlag, E. W.; Martinez, T. J.; Levine, R. D. *J. Phys. Chem. A* **1997**, *101*, 7702.

(47) Remacle, F.; Levine, R. D.; Schlag, E. W.; Weinkauf, R. *J. Phys. Chem. A* **1999**, *103*, 10149.